5th International Conference on Contemporary Problems of Thermal Engineering
CPOTE 2018, 18-21 September 2018, Gliwice, Poland
Institute of Thermal Technology

Comparative Exergy and Economic Assessment of Fossil and Biomass-Based Routes for Ammonia Production

Daniel Flórez-Orrego[a], François Maréchal[b], Silvio de Oliveira Junior[c]
[a,c] Polytechnic School, University of Sao Paulo, Department of Mechanical Engineering, Sao Paulo, Brazil,
[a]daflorezo@usp.br CA, [c]soj@usp.br,
[b] École Polytechnique Fédérale de Lausanne, Institute of Mechanical Engineering, Lausanne, Switzerland,
[b]francois.marechal@epfl.ch

The pursuit of alternative energy sources for the synthetic fertilizers sector has recently earned renewed interest due to increasing concerns regarding the marked dependence of the world economy on non-renewable energy resources, also motivated by the more stringent environmental regulations. The decarbonization of this productive sector, responsible for about 2% of the global energy consumption [1], might help not only improving the carbon footprint of these fundamental commodities, but also reducing their dependence on the international market prices, traditionally dominated by the main natural gas producers. Accordingly, in this paper, the use of biomass gasification for *partially or totally* replacing the use of methane in the integrated syngas and ammonia production plant is compared with the performance of the conventional route, typically based on steam methane reforming. However, by undertaking novel designs, additional or totally different demands can be created. Consequently, the optimal integration approach between the new chemical plant and the alternative utility systems must be updated, so that the power and steam requirements remain satisfied. To this end, a systematic framework that allows selecting the most suitable utility systems (refrigeration, waste heat recovery and cogeneration) that satisfy the minimum energy requirements (MER) with the lower resources consumption and operating cost is adopted. Moreover, the exergy analysis is used to identify the potential improvements that may remain hidden to the energy integration analysis, especially regarding the integration of reactive components and combined heat and power production (CHP) and the reduction of avoidable exergy losses.

Keywords: Renewability, Decarbonization, Exergy, Fertilizers, Energy Integration.

1. Introduction

The global supply of nitrogen fertilizers faces an increasing trend estimated in 176.5 million of tons in 2018 [2]. However, the production of these large volume inorganic chemicals, of which ammonia is an staple intermediate feedstock, entails an intensive generation of atmospheric emissions, totalizing about 353 million $t_{CO2,eq}$ in the same year [3, 4]. In order to palliate the environmental impacts that nitrogen fertilizers production is responsible for, several efforts have been addressed to incentivize the partial or total decarbonization of the ammonia supply chain. Alternative pathways of hydrogen production, such as solar or wind energy, used for electrolyzing the water and separating the nitrogen from air (cryogenic distillation, selective membranes, etc.) have been widely proposed [5]. However,

as concerns the most promising alternative energy resources for hydrogen production, the thermochemical conversion routes of biomass have shown to be the most interesting opportunity to capitalize on the underexploited biomass potential in tropical countries [6].

The earliest pressurized steam/oxygen-blown, fluidized-bed biomass gasification technology (140 MW) coupled to an ammonia synthesis unit used to run on peat and saw dust (originally designed for heavy oil gasification) [7]. It was located in the Kemira Oy ammonia plant in Oulu, Finland, during the late eighties. Eventually, due to its limited competitiveness in a volatile ammonia price market, the plant had to be shut down [8]. Hitherto, the main drawbacks of the biomass-based ammonia synthesis are still related to the high investment risk, the biomass availability and the scale-up of the gasification concept [9], as it may not fully compete with current fossil-based commercial production capacities, well above 1000 t_{NH3}/day. For the sake of comparison, 'handier' coal feedstock generally allows for gasification capacities from ten to one hundred times larger (>2000MW_{th}) than those of biomass gasification plants (<170MW_{th}). In spite of this limitation, it is expected that larger pressurized biomass gasifiers may help increasing the performance of biomass conversion process [9]. Furthermore, it must be acknowledged that large scale biomass conversion systems are not without precedent, especially in Brazil, where the estimated national production capacity of bagasse in sugarcane mills has already surpassed 190 million tons per year [10]. In fact, the largest sugarcane mills have throughputs between 0.5 to 1 million tons per year of bagasse, equivalent to the biomass required to operate a 1000 t/day ammonia plant (1.8-2.7 t_{Biom}/t_{NH3}) [6, 9, 11], even when the productive season covers typically less than half of a year [10, 12].

Additionally, unlike the well-established infrastructure and the mature technology of the conventional routes of ammonia production based on fossil fuels, better solutions for the supply management, energy conversion processes, as well as higher reliability and profitability of the renewable resources are still necessary to guarantee their competitiveness [9]. Fortunately, the technology is revisited when the access to fossil resources such as natural gas and coal is limited, mainly due to scarcity or unstable international prices [13]. Moreover, more stringent environmental regulations along with increasing concerns about the marked dependence on imported fertilizers, which renders the nation vulnerable to international markets, have led the government and research institutions to seek for the utilization of the readily available bagasse stock in the production of hydrogen and other commodities traditionally based on fossil resources [14-16]. Certainly, there are well-known applications for the residual bagasse, but gasification represents a more efficient and environmentally friendly alternative compared to current direct bagasse combustion. The economic aspects are also relevant, as the average price of bagasse oscillates around 15-20 USD per ton of wet biomass, 40% lower than the cost of the same amount of available biomass in the United States [17]. It makes bagasse one of the cheapest lignocellulosic agricultural byproducts [10, 18], not to mention that the transportation costs represent also a competitive advantage, as the bagasse is available on site [17].

Some authors performed the energy and environmental analysis of the ammonia production via biomass gasification [11, 19], either considering its integration to other chemical facilities (e.g. kraft

pulp mill) or conditioning its operability to an external electricity supply. However, a more interesting scenario in the middle term in Brazil should rather consider the energy, economic and environmental benefits of the use of the fairly available and affordable sugarcane bagasse to either partially or totally replace the natural gas in the nitrogen fertilizers production facilities (FAFEN). This is motivated by a broader assessment that projects to enable an integration of the Sao Paulo state natural gas distribution system to the State's sugar cane mills, as the former strategically goes through the area where the mills settle. Accordingly, in this paper, by applying a systematic approach, an exergy and energy integration assessment of the most suitable technologies and parameters that minimize the utilities operating costs of a conventional and various alternative syngas and ammonia production plants is presented.

2. Natural gas and Biomass-based Ammonia Production Plants

Figure 1 shows the simplified layout of a conventional configuration of the ammonia production plant based on the steam methane reforming process (SMR) [20]. Therein, a mixture of saturated natural gas (steam-to-carbon ratio, S/C 3:1) is firstly fed to an adiabatic prereformer, where heavier hydrocarbons are partially decomposed into hydrogen and carbon oxides at relatively lower temperatures (< 600°C) [21]. Next, an endothermic primary reformer (SMR, 700-800°C) in series with an autothermal reformer (ATR, 1000°C) is used to convert most of the methane feed [20].

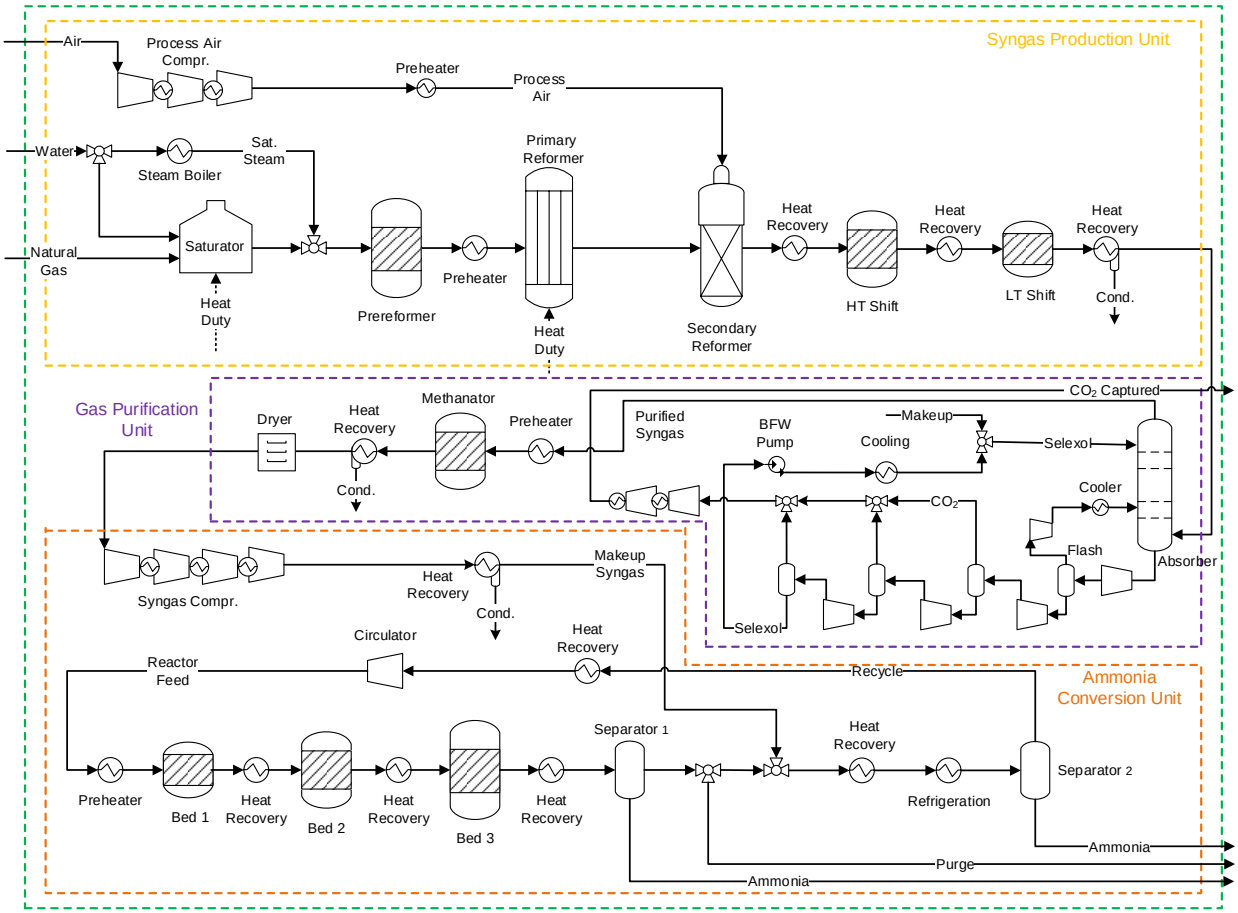

Fig.1. Conventional natural gas-fueled configuration [20].

The primary reforming is by far the most exergy-intensive processes, needing to outsource the energy required from a radiant furnace that sustains the reactions occurring in the catalytic tubes [22]. Meanwhile, in the secondary reformer, a portion of the reformed mixture is burnt with air in order to provide the energy to the endothermic reactions as well as to attain a H_2/N_2 ratio 3:1, suitable for ammonia production [23]. Downstream of the reforming sections, a set of high temperature (350°C) and low temperature (200°C) water gas shift reactors are used to further increase the hydrogen production by using the water and CO content in the reformed gas [23]. Henceforth, a purification section, composed of a physical absorption unit (DEPG) and a methanation system, is used to remove the carbon oxide components present in the syngas produced [4].

The purified syngas is then compressed up to 200 bar and fed to a synthesis loop, where the H_2/N_2 mixture is partially converted into ammonia through a series of catalytic beds indirectly cooled in order to shift the equilibrium conversion towards a higher ammonia yield [24]. The reactor performance and, consequently, the loop efficiency are affected not only by the reactor operation conditions (feed pressure, temperature and composition, heat removal and catalysts design), but also by the amount of inerts (i.e., argon and methane) and ammonia recycled. Accordingly, most of the produced ammonia must be separated by using cooling water (25-40°C) and a vapor compression refrigeration system (evaporator temperature -30°C). Moreover, in order to prevent the built up of inerts in the loop, a portion of the hydrogen-rich gas is continuously purged, whereas the rest of the unreacted mixture is recycled to the converter beds.

Meanwhile, Fig. 2 shows the process superstructure used to determine the performance of the ammonia production by using the gasification of sugar cane bagasse. The bagasse ultimate composition (mass) is set as 46.70%C, 6.02% H, 44.95% O, 0.17% N, 0.02% S and 2.14% Ash, whereas proximate analysis (mass) is considered as 50% moisture (as-received), 14.32% fixed carbon, 83.54% volatiles, and ash in balance [16]. The large moisture content of bagasse is reduced to about 10% in a rotary dryer that consumes the power and heat supplied by the utility systems, as well as the heat recovered from the gasifier effluents [25]. Bagasse must be also chipped by means of an energy intensive process that may require between 1 to 3% of the total energy embodied (LHV basis) in the biomass consumed [11].

In the gasification step, the carbonaceous materials in the bagasse are converted into a gaseous mixture called syngas, rich in CO, H_2, CO_2 and CH_4, among other components [25]. This gas can be used as process feedstock or even provide the combined heat and power required by the chemical processes, more efficiently than in biomass combustion. It is thus not surprising that gasification has gained renewed interest worldwide mainly for the production of chemicals including fertilizers, liquid fuels as well as power and gaseous fuels [13]. However, the variable biomass composition and its relatively high moisture content, along with the complex gasification operation conditions strongly influence the process yield, the energy requirement and, consequently, the efficiency of the chemical process [26, 27].

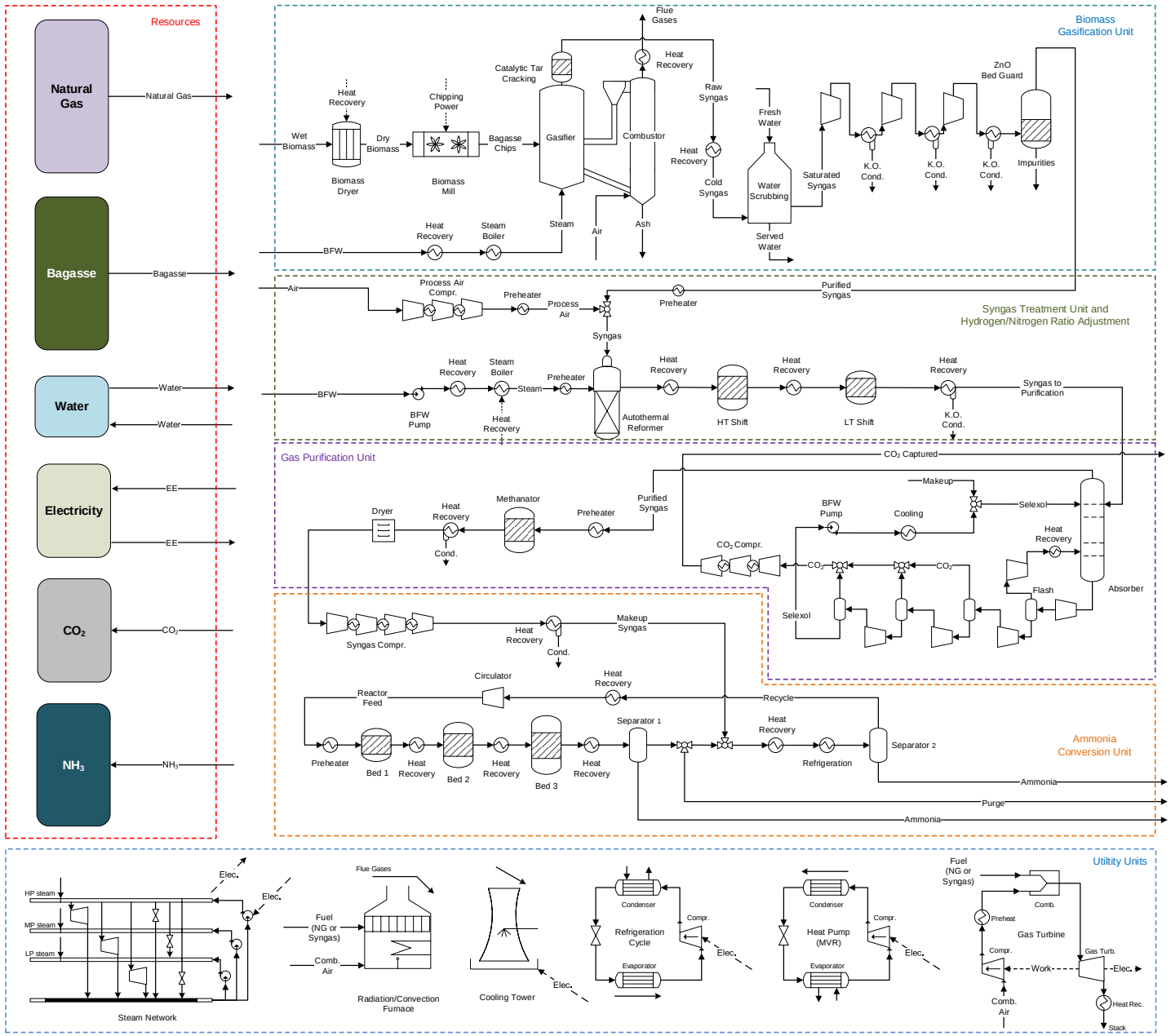

Fig. 2. Superstructure used in the process synthesis and optimization of the utility systems of the biomass-based ammonia production plant.

The Battelle Columbus Laboratory (BCL) indirect gasifier operating at atmospheric pressure, shown in Fig. 2 avoids the dilution with nitrogen of the syngas produced, as the combustion and gasification processes occur in a separate double column system [28]. Steam is used as the gasification medium (steam-to-biomass ratio 0.75), whereas the combustion with air of a fraction of the char produced in the bagasse pyrolysis step supplies the heat required by the endothermic drying, pyrolysis and reduction reactions. After the syngas produced leaves the gasifier, a thermal catalytic cracking of the tar produced is performed [29]. Then, the syngas is cooled down to 400ºC and scrubbed with water, in order to remove the impurities that may affect the downstream equipment and, then compressed to 35 bar. As long as the syngas still contains methane and carbon monoxide, an autothermal reforming and a water gas shift reaction processes, analogous to that described for the ammonia production via the conventional process, help increasing the hydrogen content, simultaneously producing more CO_2. Henceforth, the hydrogen-rich syngas can be either sent to purification for ammonia production, or used in the utility system to generate electromechanical power or to supply the heat exergy to the chemical process.

Finally, according to Fig. 2, the various alternatives of utility systems available for supplying the power and heat demands of the chemical plant include syngas or natural gas-fired furnaces and gas turbine systems, a cooling tower, a vapor-compression refrigeration system, as well as the resources consumed (e.g. natural gas, biomass, water, electricity). The cooling water inlet and outlet temperatures are set as 40°C and 25°C, respectively, and a cooling tower power-to-cooling duty ratio of 0.021 kW_{el}/kW_{th} is assumed [30]. The refrigeration system is, in turn, defined in terms of its exergy efficiency (50%) and the evaporator and condenser temperatures [20]. Additionally, the waste heat available throughout the chemical processes is recovered by using an integrated steam network, so that the amount of fuel and cooling water, necessary to balance the power and heat demands of the plant (feed preheating, endothermic reactions) can be reduced [20]. The steam network superstructure is composed of a set of superheated steam headers and draw-off levels of steam. The choice of the optimal levels of steam generation is performed by examining the profile of the Grand Composite Curve (GCC) of the chemical process [31]. In this way, more power can be generated by optimally profiting the thermodynamic potential of the waste heat exergy via backpressure and condensation steam turbines.

3. Methodology

In this section, the modeling and optimization methodology, based on a combined exergy analysis and energy integration study, is discussed.

3.1. Process modeling and overall performance indicators

The evaluation of the thermodynamic properties of each flow as well as the mass, energy and exergy balances of each unitary operation are carried out by using Aspen Plus® V8.8 software and the Peng-Robinson EOS with Boston-Mathias modifications [32]. The Perturbed-Chain Statistical Associating Fluid Theory (PC-SAFT) is used to model the physical absorption of CO_2 with dimethyl ethers of

polyethylene glycol (DEPG) as in ref. [20]. Physical and chemical exergy calculations, as well as exergy efficiencies are assessed using VBA® scripts as *user defined functions* [33].

In order to perform the material and energy balances of the bagasse pretreatment processes (drying and chipping), a FORTRAN subroutine is implemented in Aspen® Plus. The amount of moisture removed in the rotary dryer $m_{H_2O\ removed}$ (kg/h) is calculated in terms of the initial bagasse moisture $\psi_{H_2O,\ As\text{-}received}$ (%), the desired bagasse moisture at the inlet of the gasifier $\psi_{H_2O,\ Dried\ bagasse}$ (%) and the feed mass flow rate of the wet bagasse, $m_{Wet\ bagasse}$ (kg/h), according to Eq.(1):

$$m_{H_2O\ removed} = \left(\psi_{H_2O,\ As\text{-}received} - \frac{1-\psi_{H_2O,\ As\text{-}received}}{1-\psi_{H_2O,\ Dried\ bagasse}} \times \psi_{H_2O,\ Dried\ bagasse} \right) \times m_{Wet\ bagasse} \quad (1)$$

On the other hand, gasification is modeled and simulated as a series of interrelated drying, pyrolysis, reduction and combustion processes, as illustrated in Fig. 3.

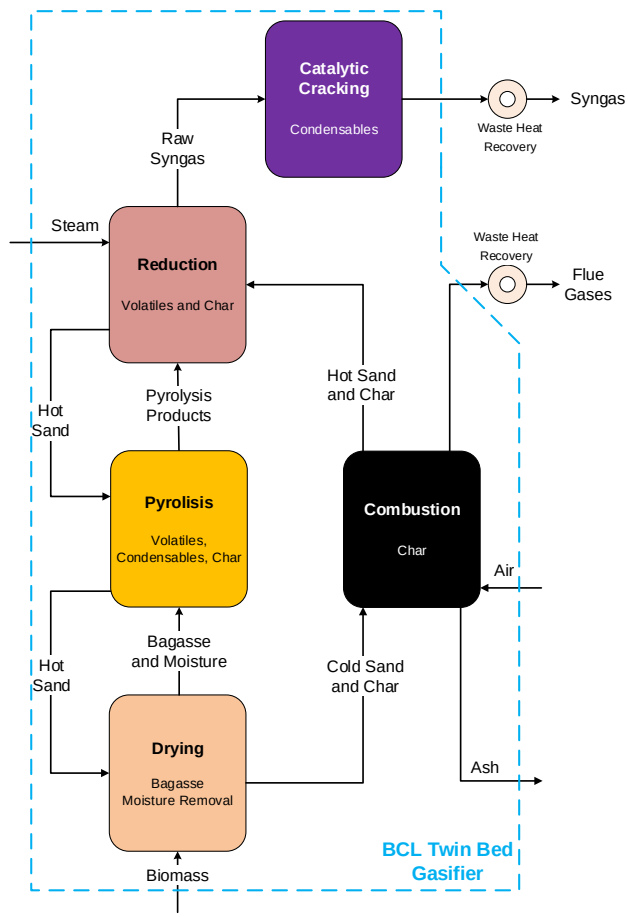

Fig. 3. Modeling and simulation steps of the twin circulated bed BCL bagasse gasifier

The actual mass yields (y_j) of volatiles, condensables, and solids in the *pyrolysis* reaction step, as well as the gaseous volumetric fractions v_i of the hydrogen, carbon monoxide, carbon dioxide, methane produced are calculated by means of a set of empirical correlations reported in the literature as a

function of the reaction temperature *T*, Eqs.(2-8) [34, 35]. To this end, an Aspen-embedded Excel® spreadsheet calculator has been used to perform the atomic balance of species (C, H, O, N, and S) comprised in the volatiles, condensables, char and ash produced in the pyrolysis section:

$$y_{Gas} = 311.10 - 351.45\left(\frac{T}{500}\right) + 121.43\left(\frac{T}{500}\right)^2 \quad \text{Gases (\%wt. of dry biomass)} \tag{2}$$

$$y_{Char} = -15.03 + 50.58\left(\frac{T}{500}\right) - 18.09\left(\frac{T}{500}\right)^2 \quad \text{Char (\%wt. of dry biomass)} \tag{3}$$

$$y_{Tar} = -196.07 + 300.86\left(\frac{T}{500}\right) - 103.34\left(\frac{T}{500}\right)^2 \quad \text{Tar (\%wt. of dry biomass)} \tag{4}$$

$$v_{CO} = 240.53 - 225.12\left(\frac{T}{500}\right) + 67.50\left(\frac{T}{500}\right)^2 \quad \text{CO (\%mol. of gas)} \tag{5}$$

$$v_{CO_2} = -206.86 + 267.66\left(\frac{T}{500}\right) - 77.50\left(\frac{T}{500}\right)^2 \quad \text{CO}_2 \text{ (\%mol. of gas)} \tag{6}$$

$$v_{CH_4} = -168.64 + 214.47\left(\frac{T}{500}\right) - 62.51\left(\frac{T}{500}\right)^2 \quad \text{CH}_4 \text{ (\%mol. of gas)} \tag{7}$$

$$v_{H_2} = 234.97 - 257.01\left(\frac{T}{500}\right) + 72.50\left(\frac{T}{500}\right)^2 \quad \text{H}_2 \text{ (\%mol. of gas)} \tag{8}$$

Additionally, aiming to correct the underestimation of the tar and methane produced (a well-known shortcoming of the non-stoichiometric equilibrium methods [25]), the approach-to-equilibrium temperatures for the char gasification and water gas shift reactions are adjusted to reflect the actual composition of the syngas produced in the BCL gasifier [36, 37]. Meanwhile, the ratio of specific chemical exergy to the lower heating value is calculated by means of the correlation proposed by Szargut et al [38] for solid fuels with specified mass ratios, Eq.(9).

$$\beta = \frac{b^{CH}}{LHV} = \frac{1.0438 + 0.1882 \cdot \frac{y_H}{y_C} - 0.2509\left(1 + 0.7256 \cdot \frac{y_H}{y_C}\right)}{1 - 0.3035 \cdot \frac{y_O}{y_C}} \tag{9}$$

where the bagasse lower heating value (LHV, MJ/kg) is estimated based on the correlations reported by Channiwala et al. Eq.(10) [39]:

$$LHV = 349.1 \cdot y_C + 1178.3 \cdot y_H + 100.5 \cdot y_S - 103.4 \cdot y_O - 15.1 \cdot y_N - 21.1 \cdot y_{Ashes} - 0.0894 \cdot hlv \cdot y_H \tag{10}$$

and y_i are the mass fractions of carbon (C), hydrogen (H), sulfur (S), oxygen (O), nitrogen (N) and ashes (A) in the dry biomass, and h_{lv} is the enthalpy of evaporation of water at standard conditions (2442.3 kJ/kg). The so-calculated lower heating value and chemical exergy of dry bagasse are equal to 17.3 and 19.5 MJ/kg, respectively.

3.2. Exergy efficiency definition

Some performance indicators for each ammonia plant configuration are proposed to allow for systematic comparisons between the different designed setups, based on ***totally and partially natural gas-fueled, and totally biomass fueled ammonia plants with and without electricity import***. Table 1 compares the *rational* exergy efficiency, Eq. (11), with other exergy efficiency definition, Eqs.(12), proposed for evaluating the overall performance of chemical production plants [4]. It must be noticed that, the rational exergy efficiency is higher than the relative one as it accounts for the outlet exergy of other byproducts (CO_2, purge gas).

Table 1. Plantwide exergy efficiency definitions of the ammonia production plants.

Definition	Formula	Equation
Rational	$\eta_{\text{Rational}} = \frac{B_{useful,output}}{B_{input}} = 1 - \frac{B_{Dest}}{B_{input}} = 1 - \frac{B_{Dest}}{B_{CH_4} + B_{Bagasse} + B_{BFW} + W_{Net}^{Import}}$	(11)
Relative	$\eta_{\text{Relative}} = \frac{B_{consumed,\,ideal}}{B_{consumed,\,actual}} = \frac{B_{Ammonia}}{B_{CH_4} + B_{Biomass} + B_{BFW} + W_{Net}^{import}}$	(12)

B = exergy rate or flow rate (kW), BFW = boiler feedwater, Dest = destroyed.

3.3. Optimization problem definition

As it has been shown hitherto, ammonia production plants are designed in complex ways in which the chemical units and the processes streams are interrelated through recycle loops and an extensive waste heat recovery network. Moreover, as long as the electricity can be imported from the grid, there is a trade-off between the use of an additional amount of fuel in the cogeneration system and the extent of the electricity purchase. Actually, since both resources can be used to supply the power demand of the whole plant, the choice will be strongly influenced by the performance of the cogeneration and waste heat recovery systems [40], as well as by the ratio between the cost of the electricity and the fuels consumed [41]. Furthermore, since the conventional process flowsheet is drastically modified when alternative energy resources are considered, additional or totally different demands may be created. This requires a complete redesign of the energy integration approach between the new chemical units and the redefined utility systems, so that the power and steam requirements remain satisfied.

For instance, biomass can be chosen to either totally or partially replace the natural gas as feedstock, as fuel or as both, opening an opportunity to the diversification of the input of the chemical systems, depending on the availability and cost of the energy resources. In this way, cheaper energy resources, such as bagasse may be favored over more expensive energy inputs [42]. Moreover, by importing electricity in lieu of generating it in the utility systems, the energy, economic and environmental impacts are transferred to the outside of the battery limits. Thus, depending on the electricity mix, it may bring more energy and environmental benefits than using natural gas in the cogeneration system. All these new features render the determination of the optimality a cumbersome task. It must be also

noticed that the energy integration method alone falls short to put on evidence the exergy destruction in the heat exchanger network and reveal the potential for reducing the inherent driving forces by rationally performing the waste heat recovery and power generation. Fortunately, the selection of the most suitable alternatives of a set of proposed energy technologies for the utility systems allows reshaping the integrated curves of the chemical process aiming to minimize the exergy destruction. This procedure relies on an efficient mathematical programming approach in which all the potential energy technologies, resources and production routes are included in a comprehensive superstructure. Additionally, by separating the chemical process simulation from the energy integration problem, the calculation of the mass and energy balances and the simulation of the complex energy conversion systems can be handled by using the Aspen® Plus modeler [43]. Meanwhile, the determination of the minimum energy requirements (MER) and the solution of the energy integration problem is handled by the OSMOSE Lua platform, developed by the IPESE group at the École Polytechnique Fédérale de Lausanne - EPFL, Switzerland [44].

In order to calculate the minimum energy requirement (MER), the contribution of each hot and cold streams to the overall heat balance is combined into the respective hot and cold composite curves [45]. These composite curves are shifted away from each other through a physical constraint, namely the minimum temperature approach ΔT_{min}, so that reasonable heat transfer rates can be ensured. Clearly ΔT_{min} will depend on the nature of each stream [46]. Equation (13-15) shows the optimization problem set to find the MER:

$$\min_{R_r} R_{N_r+1} \tag{13}$$

Subject to

Heat balance of each interval of temperature r $$\sum_{i=1}^{N} Q_{i,r} + R_{r+1} - R_r = 0 \qquad \forall r = 1 \,..\, N \tag{14}$$

Feasibility of the solution $$R_r \geq 0 \tag{15}$$

where N is the number of temperature intervals defined by considering the supply and the target temperatures of the entire set of streams; Q is the heat exchanged between the process streams ($Q_{i,r} > 0$ hot stream, < 0 cold stream) and R is the heat cascaded from higher *(r+1)* and to lower *(r)* temperature intervals (kW).

This framework also allows to determine the most suitable utility systems (e.g. steam network, refrigeration system, heat pump, cogeneration system) and their operating conditions, that satisfy the minimum energy requirement (MER) with the lowest resources consumption (water, natural gas and bagasse) and optimal operating cost [45]. The computational framework manages the data transfer with the ASPEN Plus® software and builds the mixed integer linear programming (MILP) problem described in the Eqs.(16-20) that minimizes the operating cost of the chemical plant. In other words, the optimization problem consists of finding the integer variables, y_w, associated to the existence or

absence of a given utility unit, ω, and its corresponding continuous load factor, f_w, that minimizes the objective function given by Eq.(16):

$$\min_{\substack{f_\omega,\ y_\omega \\ R_r, W}} \left[\begin{array}{l} f_{CH_4}^{resource}\left(B\cdot c\right)_{CH_4} + f_{Biomass}^{resource}\left(B\cdot c\right)_{Biomass} + f_{Water}^{resource}\left(V\cdot c\right)_{Water} + f_{Power}^{resource}\left(W\cdot c\right)_{Power}^{import} \\ \qquad\qquad - f_{NH_3}^{resource}\left(B\cdot c\right)_{NH_3} - f_{CO_2}^{resource}\left(\dot{m}\cdot c\right)_{CO_2} \end{array} \right] \quad (16)$$

Subject to:

Heat balance of temperature interval r $$\sum_{\omega=1}^{N_\omega} f_\omega q_{\omega,r} + \sum_{i=1}^{N} Q_{i,r} + R_{r+1} - R_r = 0 \qquad \forall r = 1..N \quad (17)$$

Balance of produced/consumed power $$\sum_{\omega=1}^{N_\omega} f_\omega W_\omega + \sum_{\substack{chemical \\ units}} W_{net} + W_{imp} - W_{\exp} = 0 \quad (18)$$

Existence and size of the utility unit w $$f_{\min,\omega} y_\omega \le f_\omega \le f_{\max,\omega} y_\omega \qquad \forall \omega = 1..N_\omega \quad (19)$$

Feasibility of the solution (MER) $$R_1 = 0,\ \ R_{N_r+1} = 0,\ \ R_r \ge 0 \ \text{ and } \ W_{imp} \ge 0,\ W_{\exp} \ge 0 \quad (20)$$

where N_w is the number of units in the set of utility systems; B is the exergy flow rate (kW) of the resources going in and out of the plant; c stands for the purchasing cost (euro per kWh, m^3 or kg/h) of the feedstock and electricity consumed or the selling price of the marketable ammonia and CO_2 produced; V is the flowrate of water consumed (m^3/h); q is the heating/cooling rates supplied by the utility systems (kW); W is the power produced by either the utility systems, the same chemical process or imported from/exported to the grid (kW). It is important to emphasize that the process modeling and simulation of the chemical plant alone, including its mass and energy balances, is performed by using Aspen ® Plus software. Meanwhile, the utility units shown in Fig. 2 are modeled via equation oriented subroutines written in the Lua programming language. Therefore, the additional equations required for the mass and energy balances of those units rely on the concept of layer (water, natural gas, biomass, syngas, ammonia, power, carbon dioxide, heat, etc.) as shown in Fig. 4. According to Eq.(18), the overall power generated by the utility systems (steam or gas power cycles) should be able to supply the demands of the chemical plant and other utility units (refrigeration, heat pump, cooling tower). Otherwise, the balance of the respective layer considers the possibility of importing electricity from the grid. Moreover, if a surplus of power could be produced at expense of the waste heat exergy available through all the plant, the excess electricity could be sold to the grid, provided that its export is economically attractive. Analogously, in the layer of natural gas (or other resource), the amount of energy supplied by the vendors is balanced with the fuel or feedstock consumption by the chemical plant and utility systems (gas turbine, furnace). In this way, not only the balances of the resources consumed (power, natural gas, biomass, water) and the products and byproducts (ammonia, syngas, hydrogen, CO_2), but as well as of the waste heat recovered, can be performed. To this end, representative market cost for the water (3.69 euro/m^3), bagasse (0.0056 euro/kWh), natural gas consumed (0.032 euro/kWh) and electricity (0.108 euro/kWh), as well as the selling prices of ammonia (0.098 euro/kWh) and CO_2 (0.0084 euro/kWh) produced are taken from sorted literature [10, 20, 47].

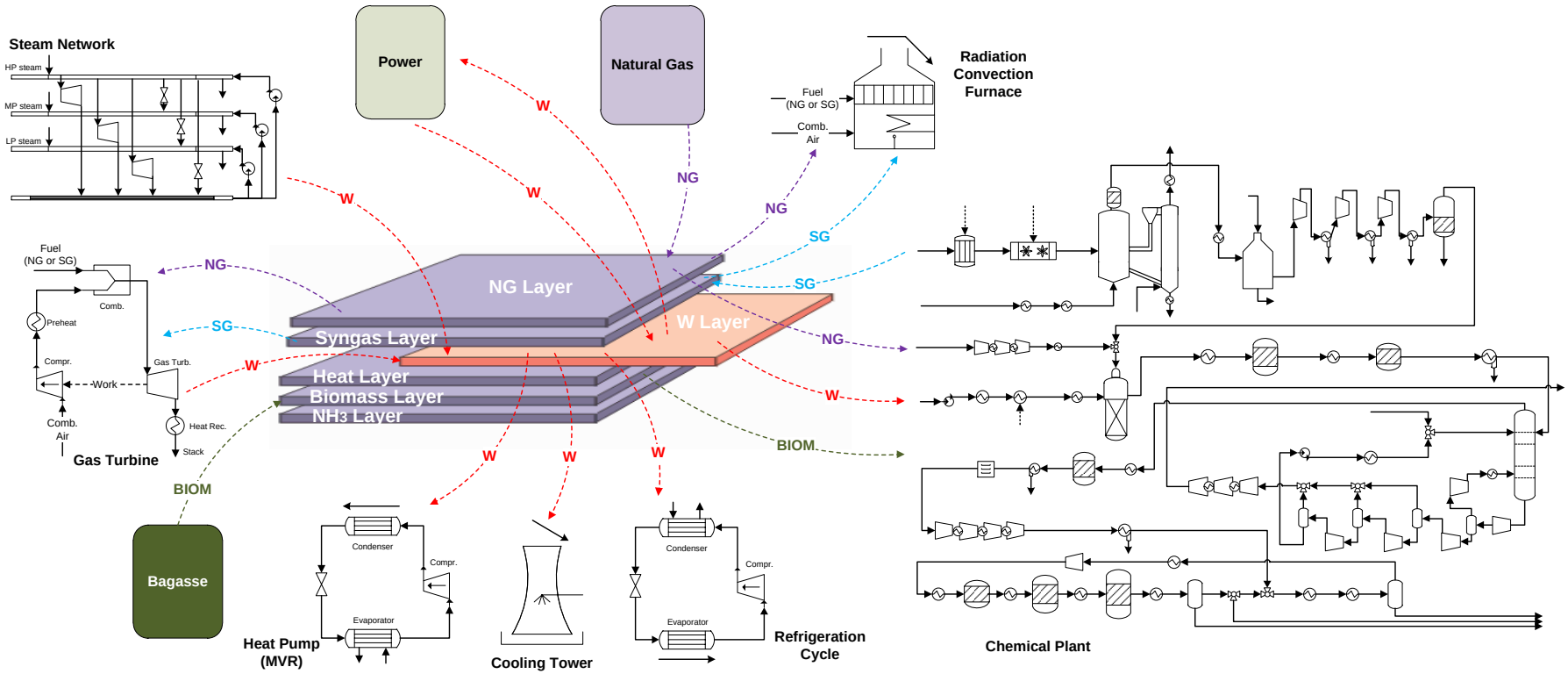

Fig. 4. Concept of layer used in the optimization of the utility systems. W: power, NG: Natural Gas, BIOM: Biomass, SG: Syngas.

4. Results and discussion

In this section, the energy consumption remarks and the performance of the optimized ammonia production setups are compared. First, it is important to notice that, unlike the conventional route that only consumes methane, the biomass-derived syngas is used as the main process feedstock for hydrogen production in the alternative configurations studied. Meanwhile, natural gas can be still consumed in the fired furnace for balancing the heating requirements in the alternative ammonia production facilities. Natural gas can be also fed to a gas turbine system in order to supply the power required to drive the compressors and pumps, as well as the cooling tower and the vapor compression refrigeration systems. As concerns the cases of total substitution of natural gas, a fraction of the biomass-derived syngas is consumed instead of importing natural gas, which directly affects the ammonia yield and, most importantly, the overall balance of the combined heat and power production of the plant. The decision making is therefore not a trivial problem, as it involves the iterative adjustment of the energy integration results [48]. Thus, by using a systematic optimization framework, the waste heat available for cogeneration purposes can be thoroughly exploited, whereas minimizing the operating cost of the plant and maximizing the total amount of ammonia produced.

4.1. Exergy consumption remarks

Apart from the conventional case using only natural gas as both feedstock and fuel (Fig. 1), thirteen additional scenarios have been tested in which the biomass-derived syngas is used as the main *feedstock* for ammonia production, but the input to the utility systems may vary according to economic and environmental targets (Fig. 2). These scenarios combine the utilization of various energy resources in the utility systems (i.e. imported natural gas, electricity from the grid, as well as produced syngas) together with the integration of either Rankine or Combined cycles. Nevertheless, only six out of all the thirteen combinations considered were found to be independent optimal solutions, namely:

Conventional case: the natural gas imported is used as both feedstock and fuel, without electricity import;
WF-RC-EE case: No gaseous fuels are consumed in the utility systems, thus, the imported electricity [49] along with the optimized steam network and Rankine cycle are responsible for the combined heat and power production;
NG-RC-no EE case: Only imported natural gas is consumed as fuel in the utility systems, whereas the optimized steam network and a Rankine cycle provide the required heat and power demands, without any electricity import required;
NG-CC-no EE case: Analogously to the previous case, except for the consumption of the natural gas imported in a more efficiency Combined cycle that supply the required heat and power demands of the chemical plant;
SG-RC-no EE case: Differently from the previous cases, here a fraction of the gasification syngas is consumed as fuel whereas an optimal steam network and a Rankine cycle provide the required heat and power demands, without the need of electricity or natural gas import;

SG-CC-no EE case: Similar to the previous case, except for the integration of a Combined cycle that consumes the syngas produced.

For instance, by enabling the natural gas turbine system (e.g. Combined cycle) while the electricity import is not allowed (see case NG-CC-noEE), the optimization solution is found to be equivalent to that of another scenario in which, even if the electricity consumption is now enabled, the optimizer still favors the natural gas consumption in a combined cycle over the import of costly electricity from the grid (i.e. NG-CC-EE).

Table 2 summarizes the results of the optimal process variables for the ammonia production scenarios considered. Moreover, according to Fig. 5, the *non-renewable* exergy consumption in the conventional case achieves 32.34 GJ/t_{NH3}, with combined CO_2 production (i.e. CO_2 in the fumes and the raw syngas) of 1.75 t_{CO2}/t_{NH3}, out of which 29.3% are not captured and, thus, emitted to atmosphere (cf. Fig. 6). The source of these emissions is related to the use of natural gas in the fired furnace of the primary reformed. Nevertheless, the conventional case presents the lowest exergy consumption among all the analyzed configurations, due to the higher operating pressures of the primary reformer when compared to the atmospheric gasification processes.

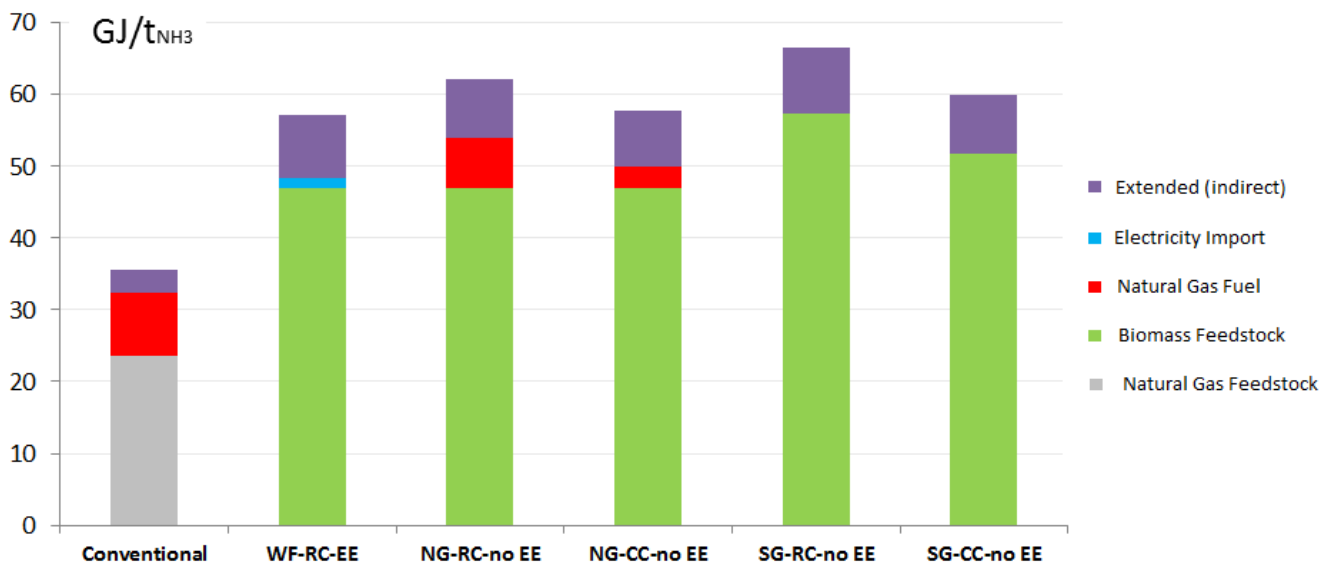

Fig. 5. Plantwide and extended exergy consumption figures for the various configurations studied.

In fact, in the biomass-based setups, the water-scrubbed syngas must be further compressed, not to mention the large amount of exergy consumed in the bagasse treatment process, which renders the biomass-based route more power intensive (see Fig. 7). The conventional case also presents the lowest overall power consumption (2.49 GJ/t_{NH3}), 60% lower than the highest power consumption figure (6.4 GJ/t_{NH3}) corresponding to the case in which only syngas is used as the fuel source for the combined heat and power generation in a steam power cycle (SG-RC-no EE).Thus, it is not surprising that the SG-RC-noEE case also accounts for the highest overall exergy input (57.32 GJ/t_{NH3}).

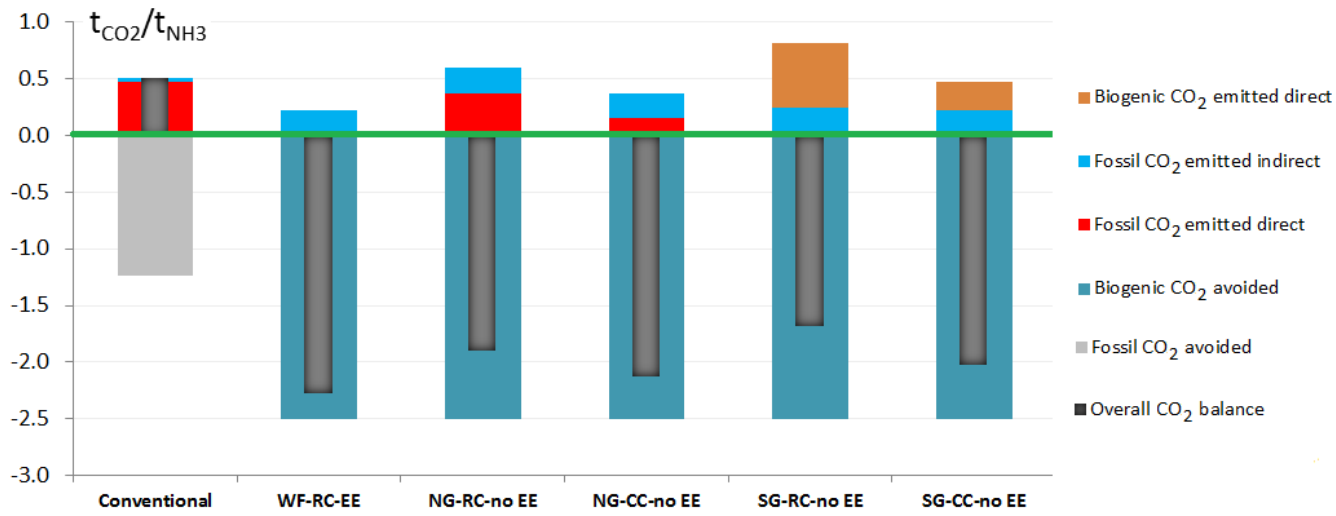

Fig. 6. Overall and detailed (biogenic and fossil, directly and indirectly emitted, and avoided) CO_2 emissions for the various configurations studied.

From Table 2, it is also evidenced that even for a higher specific consumption of feedstock, cheaper biomass input allows for a lower operating cost and, thus, higher operating revenues than if the utility system were fueled with costly natural gas. This fact explains why the lowest amount of operating revenues corresponds to the conventional case, in which natural gas is used as both feedstock and fuel. As a conclusion, the use of cheaper energy resources as well as the diversification of the energy inputs to the ammonia plant may serve not only for reducing the amount of emissions produced but also increasing the revenues obtained, even at expense of lower efficiencies (see Section 4.2) [42].

Additionally, Table 2 shows the *Extended Exergy Plant Consumption* that takes into account the exergy efficiency of the electricity generation (55.68%), as well as of the natural gas (91.09%) and bagasse (86.13%) supply chains [49]. Certainly, by adding the upstream inefficiencies in the feedstock supply chains into the originally standalone ammonia plant analysis, the panorama is worsened as the exergy destroyed in the feedstock acquisition further impairs the global performance of the production process. Accordingly, the increase in the overall exergy consumption is not negligible, varying from 15.3-17.9% in the case of the biomass-based routes (due to the larger amount of biomass required), but as low as 9.7% in the case of the conventional plant scenario, thanks to the higher exergy content of the feedstock and the conversion efficiency of the latter route. Although these figures may not be immediately interesting for ammonia producers when evaluating the performance of the plant itself, those figures certainly prove to be useful to public policy and decision makers in both environmental and benchmarking frameworks, since they allow to holistically compare the impact of the fertilizers sector with other industrial activities from a fair level playing field.

Table 2. Optimal process variables of the studied ammonia production facilities. WF: no fuel, NG: Natural Gas fuel, SG: Syngas fuel, EE: Electricity consumption, RC: Rankine cycle, CC: Combined cycle, no-EE: No electricity import.

Process parameter	Conventional	WF-RC-EE	NG-RC-no EE	NG-CC-no EE	SG-RC-no EE	SG-CC-no EE
Feedstock input	Natural Gas	Biomass	Biomass	Biomass	Biomass	Biomass
Utility system input	Natural Gas	Electricity	Natural Gas	Natural Gas	Syngas	Syngas
Cogeneration system	Rankine	Rankine	Rankine	Combined	Rankine	Combined
Feedstock consumption (GJ/t_{NH3})	23.51	47.04	47.04	47.04	57.32	51.66
Utility fuel consumption (GJ/t_{NH3})	8.83	0.00	6.90	2.91	6.79[10]	3.05[10]
Utility electricity consumption (GJ/t_{NH3})	0.00	1.41	0.00	0.00	0.00	0.00
Overall plant consumption (GJ/t_{NH3})	**32.34**	48.45	53.95	49.95	**57.32**[10]	51.66[10]
Extended plant consumption (GJ/t_{NH3}) [1]	**35.49**	57.15	62.19	57.81	**66.55**	59.98
Rankine cycle power generation (GJ/t_{NH3})[2]	**2.49**	4.22	5.73	4.32	**6.40**	4.53
Brayton cycle power generation (GJ/t_{NH3})[2]	0.00	0.00	0.00	1.33	0.00	1.43
Chemical process power demand (GJ/t_{NH3})[3]	**1.81**	4.88	4.88	4.88	**5.56**	5.19
Ancillary power demand (GJ/t_{NH3})[4]	0.68	0.75	0.85	0.77	0.84	0.77
Cooling requirement (GJ/t_{NH3})[5]	5.86	10.92	10.91	10.92	10.95	10.93
Heating requirement (GJ/t_{NH3})[5]	2.13	0.00	0.00	0.00	0.00	0.00
Fossil CO_2 emissions avoided (t_{CO2}/t_{NH3})[6]	1.237	0.000	0.000	0.000	0.000	0.000
Fossil CO_2 emitted –direct (t_{CO2}/t_{NH3})	0.470	0	0.368	0.155	0.000	0.000
Fossil CO_2 emitted – indirect (t_{CO2}/t_{NH3})[7]	0.043	0.227	0.236	0.217	0.246	0.222
CO_2 emitted indirect – EE grid (%)	0.00	10.74	0.00	0.00	0.00	0.00
CO_2 emitted indirect – Nat. Gas (%)	100.00	0.00	14.33	6.58	0.00	0.00
CO_2 emitted indirect – Bagasse (%)	0.00	89.26	85.67	93.42	100.00	100.00
Total fossil CO_2 emitted (t_{CO2}/t_{NH3})	0.513	0.227	0.604	0.372	0.246	0.222
Biogenic CO_2 emissions avoided (t_{CO2}/t_{NH3})[6]	0.000	2.503	2.503	2.503	2.503	2.503
Biogenic CO_2 emitted – direct (t_{CO2}/t_{NH3})	0.000	0.000	0.000	0.000	0.569	0.256
Total atmospheric emissions (t_{CO2}/t_{NH3})	0.513	**0.227**	0.604	0.371	**0.816**	0.478
Overall CO_2 emissions balance[8]	**0.513**	**-2.276**	-1.899	-2.131	-1.687	-2.025
Biomass consumption ($t_{Bagasse}/t_{NH3}$)	--	2.41	2.41	2.41	2.94	2.65
Gasifier syngas production (GJ/t_{NH3})	--	31.06	31.06	31.06	37.85[10]	34.11[10]
Operating Incomes[9] (euro/t_{NH3})	516.72	529.34	529.34	529.34	529.98	529.63
Operating Costs[9](euro/t_{NH3})	281.05	107.59	124.73	90.31	79.53	71.67
Operating Revenues[9] (euro/t_{NH3})	**235.67**	421.75	404.62	439.04	450.45	**457.96**
Ammonia production (t/day)	950.84	1119.22	1119.22	1119.22	918.45[10]	1019.14[10]

1. Overall exergy consumption increases if the extended efficiency of the electricity grid (55.67%), natural gas (91.09%) and bagasse (86.13%) supply are considered as in ref. [49, 50]; 2. Steam pressure levels 110, 25, 2.5 and 0.10 bar, steam superh. 200°C, Brayton cycle with regeneration, pressure ratio 20:1; 3. Power consumed by the chemical plant alone; 4. Cooling tower and vapor compression refrigeration systems; 5. Heating and cooling requirements of the chemical processes (energy basis) determined from the composite curves; 6. CO_2 emissions captured through the physical absorption system; 7. It considers the indirect emissions due to the upstream supply chains of natural gas (0.0049 g_{CO2}/kJ_{CH4}), electricity (62.09 g_{CO2}/kWh) and residual bagasse (0.0043 $g_{CO2}/kJ_{Bagasse}$) [49, 50]; 8. It considers the overall CO_2 emitted (either fossil or biogenic) minus biogenic CO_2 captured; 9. Operating revenues (only) calculated as the difference between the gross operating incomes minus the operating cost; 10. It considers bagasse as the only energy input of the ammonia plant, thus the utility fuel consumption is a fraction of the syngas produced, which also reduces the amount of ammonia produced.

Furthermore, the indirect emissions related to the supply chains of the electricity, natural gas and bagasse (production, distribution, etc.) have been included in the calculation of the actual CO_2 fossil emitted in Table 2 [49, 50]. Such indirect contribution is not negligible and reveals environmental issues that otherwise may remain hidden if the electricity imported is considered as an *emissions-free* input. For instance, the indirect emissions of the bagasse supply are the largest share of indirect emissions (85-100%) in the biomass-based route (0.23 t_{CO2}/t_{NH3}). This value is on average fivefold the indirect emissions associated to the conventional route (0.043 t_{CO2}/t_{NH3}) and can be explained by the large amount of bagasse required, which not only takes a toll to the efficiency of the overall plant, but also proportionally increases the indirect emissions produced. Thus, if the biomass resource is not available on site and requires large distance ship, train or truck transportation systems, e.g. from tropical to non-tropical countries, a higher carbon footprint of the entire ammonia production could be expected due to the increased indirect emissions.

On the other hand, the direct emissions are derived from the combustion of natural gas or raw syngas (with an important biogenic CO_2 content), used to supply the combined heat and power production. Meanwhile, the avoided emissions are related to the carbon capture system in the syngas purification section. Since direct biomass-derived CO_2 emissions are considered as neutral emissions [51], the difference between the biogenic CO_2 captured and the overall CO_2 emitted is considered as the balance of CO_2 emissions (see Table 2). The negative value indicates an overall positive impact in the depletion of CO_2 present in the atmosphere, meaning that for each ton of ammonia produced, between 1.7 to 2.3 tons of CO_2 are withdrawn from the environment. This is in close agreement with reported literature [19]. As a result, the indirect emissions from the bagasse utilization are not only offset by the captured biogenic emissions, but also the import of 'greener' Brazilian electricity (WF-RC-EE) leads to the best results in terms of overall exergy consumption and CO_2 emissions among the *partially and totally renewable* routes analyzed in Table 2.

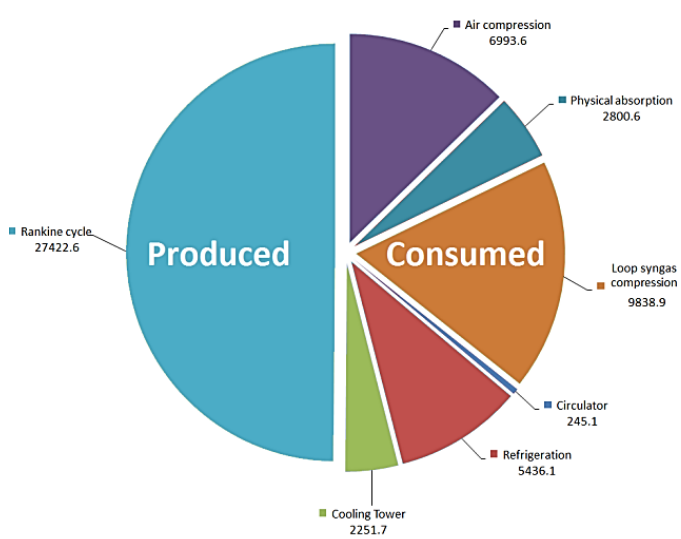

Rankine cycle steam pressure levels 110, 40, 3, 0.12 bar, steam superh. 200°C, no EE import, natural gas fuel

(a)

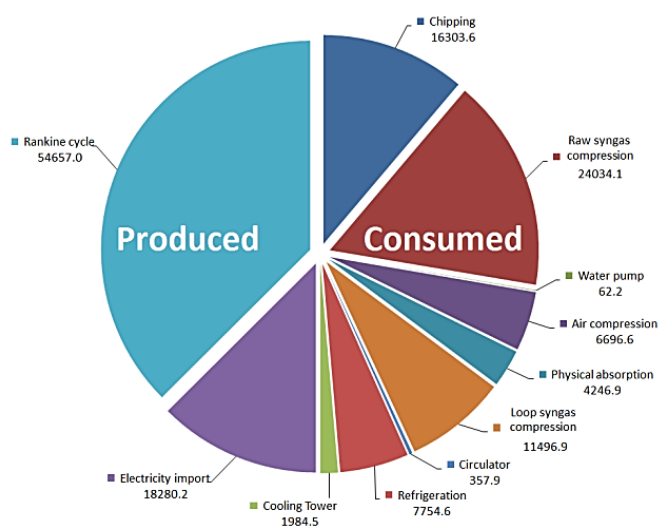

Rankine cycle steam pressure levels 110, 25, 2.5, 0.10 bar, steam superh. 200°C, EE import, no fuels

(b)

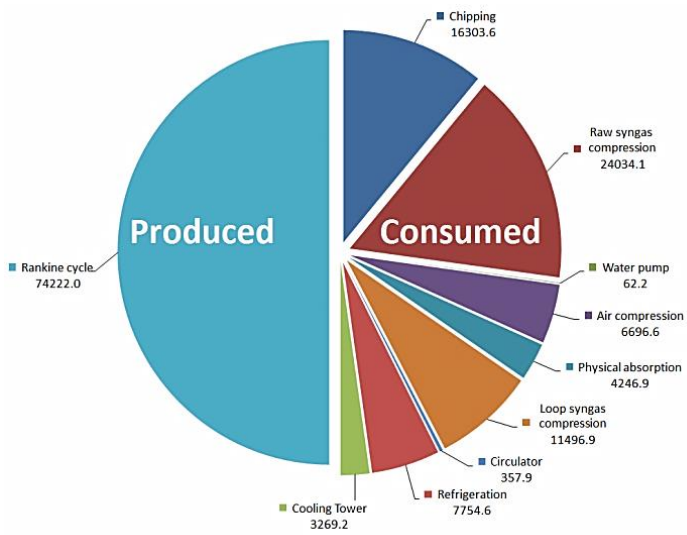

Rankine cycle steam pressure levels 110, 25, 2.5, 0.10 bar, steam superh. 200°C, no EE import, natural gas fuel

(c)

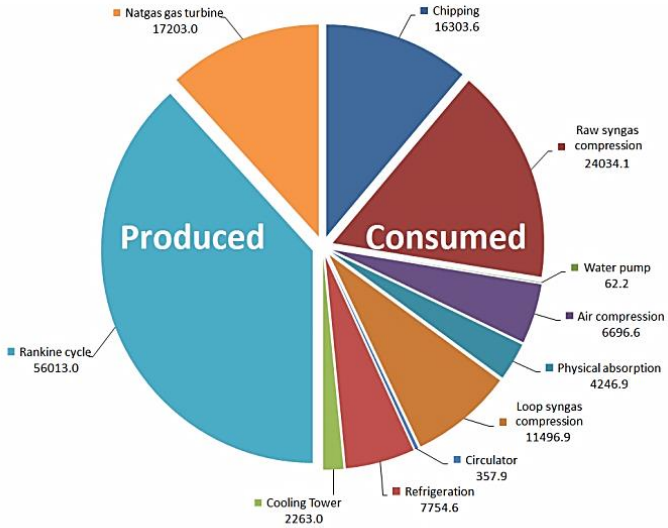

Combined cycle steam pressure levels 110, 25, 2.5, 0.10 bar, steam superh. 200°C, no EE import, natural gas fuel, gas turbine 20:1 bar

(d)

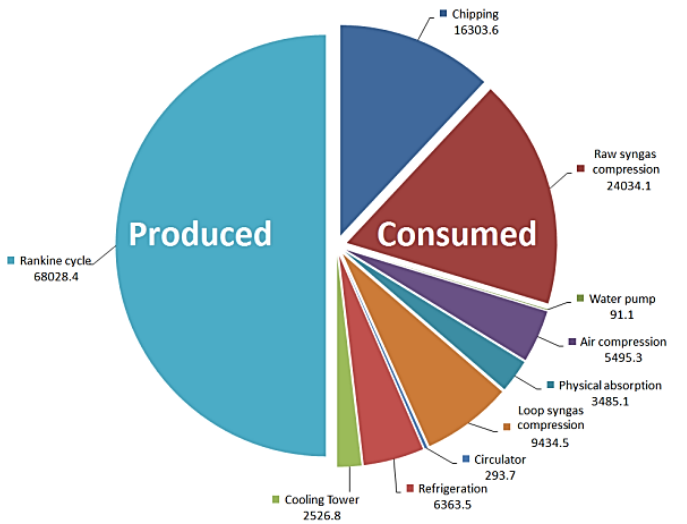

Rankine cycle steam pressure levels 110, 25, 2.5, 0.10 bar, steam superh. 200°C, no EE import, syngas fuel

(e)

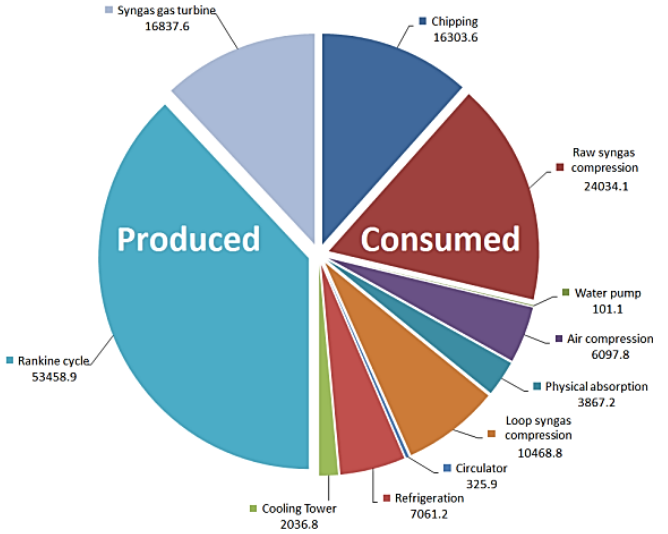

Combined cycle steam pressure levels 110, 25, 2.5, 0.10 bar, steam superh. 200°C, no EE import, syngas fuel, gas turbine 20:1 bar

(f)

Fig. 7. Power consumption breakdown of the selected scenarios, EE: electricity, superh.: steam superheating, (a) Conventional, (b) WF-RC-EE, (c) NG-RC-no E, (d) NG-CC-no EE,(e) SG-RC-no EE, (f) SG-CC-no EE, see also Table 2.

4.2. Energy integration and Exergy Analyses

Figure 8a-f show the integrated curves corresponding to the simulated scenarios described in Table 2.

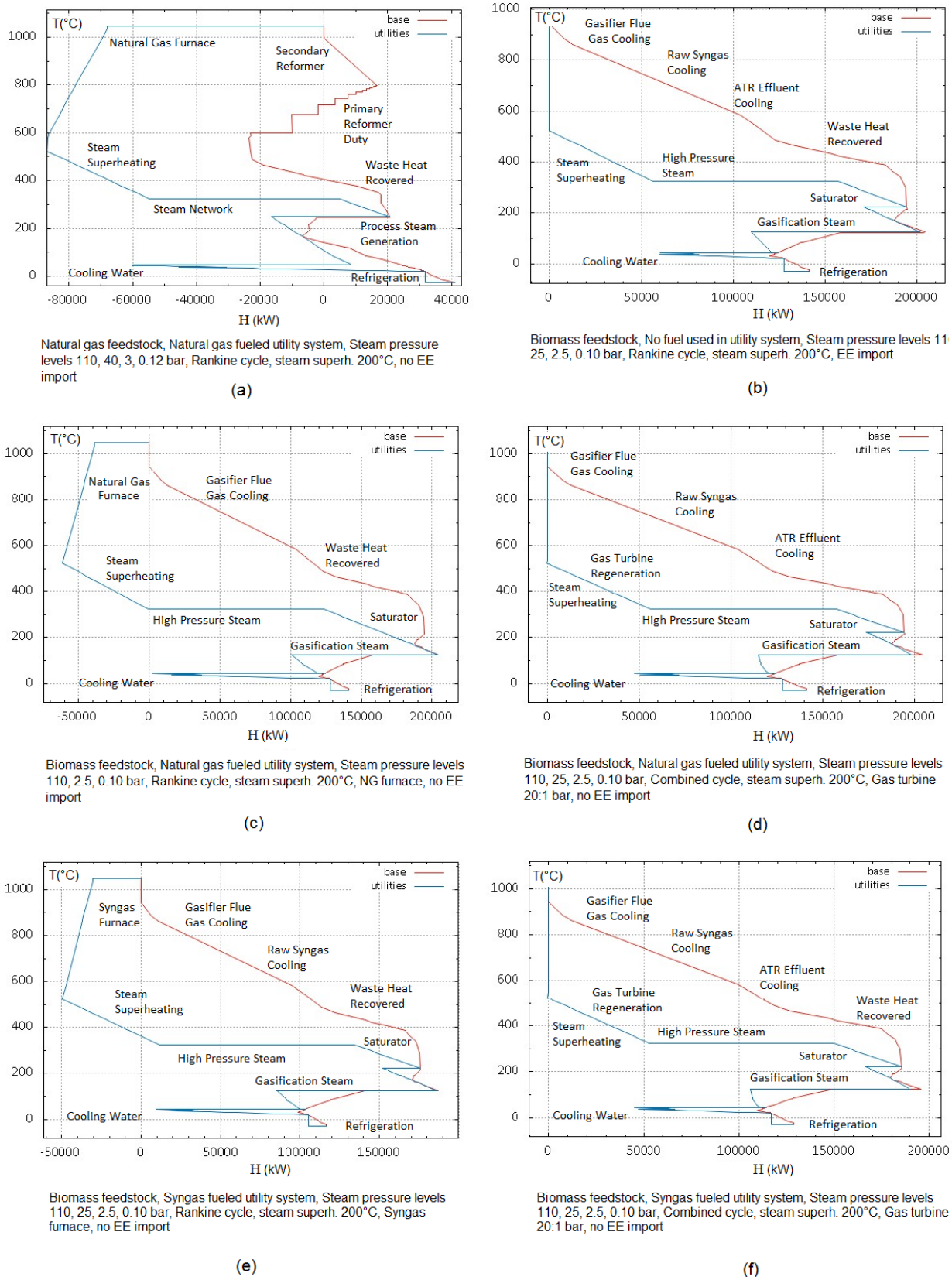

Fig. 8. Integrated composite curves. EE: electricity, superh.: steam superheating, (a) Conventional, (b) WF-RC-EE, (c) NG-RC-no E, (d) NG-CC-no EE,(e) SG-RC-no EE, (f) SG-CC-no EE, cf. Table 2.

As it can be observed, the bagasse-based ammonia production designs, *Figs. 8* (b-c) present a higher potential of heat recovery due to the excess heat exergy available throughout the whole chemical plant. This is profited by integrating a steam network that recovers and then supplies the heat required, either by preheating process streams or by raising steam (used as both process reactant and power fluid).

On the other hand, the reduced excess heat exergy available in the conventional case (Fig. 8a) must be compensated by an increased consumption of fuel in the utility system, about 21 to 84% higher than in the cases (b-c). In spite of this fact, the share of exergy destruction in the natural gas-fired furnace and the primary reformer together (6.7 GJ/t_{NH3}) is still much lower than the sum of the irreversibility comprised in the bagasse treatment (chipping, drying, scrubbing), gasification and syngas compression processes together, according to Fig. 9 and Table 3. Actually, the latter irreversibility accounts for approx. 16.2 GJ/t_{NH3} or 60-80% of the exergy destroyed in the bagasse-based ammonia production setups. The gasifier itself is responsible for half of the exergy destruction in the plant and, as the char combustion process is inevitable, there is a small room for reducing its contribution to the total process irreversibility. However, as concerns the drying, chipping and cold syngas cleaning (water scrubbing), and compression processes, better technologies for the removal of the bagasse moisture, hot catalytic cleaning of the syngas and increased gasifier pressures may help reducing the amount of avoidable exergy destroyed in the frontend of biomass-based ammonia production plants [29].

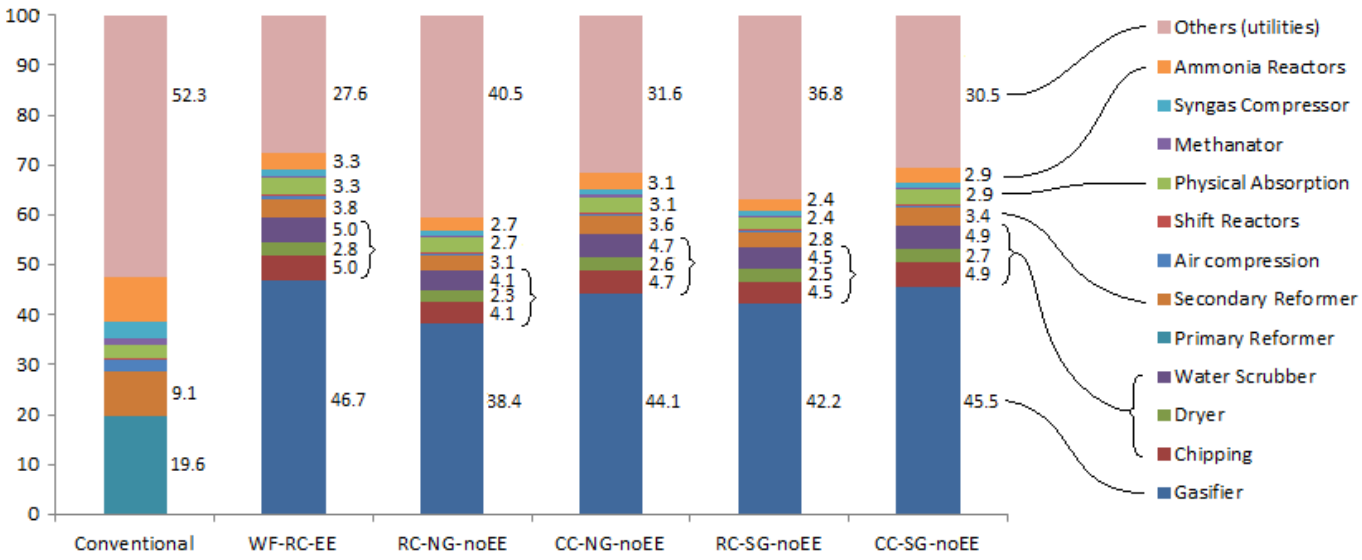

Fig. 9. Exergy destruction breakdown for the selected scenarios, EE: electricity, superh.: steam superheating, (a) Conventional, (b) WF-RC-EE, (c) NG-RC-no E, (d) NG-CC-no EE,(e) SG-RC-no EE, (f) SG-CC-no EE, see Table 2.

The calculated plantwide rational efficiencies shown in Table 3 are in close agreement with those reported for the thermo-environonomic optimization of two biomass and natural gas-based ammonia production plants with electricity import [19].

Table 3. Exergy destruction and exergy efficiencies for the studied configurations

Process parameter	Conventional	WF-RC -EE	NG-RC -no EE	NG-CC -no EE	SG-RC -no EE	SG-CC -no EE
Rational exergy efficiency (%)	70.17	47.87	42.99	46.43	40.46	44.89
Extended rational exergy efficiency (%)[1]	63.92	40.58	37.29	40.12	34.85	38.67
Relative exergy efficiency (%)	**61.47**	41.02	36.85	39.79	**34.67**	38.47
Extended relative exergy efficiency (%)[1]	**56.00**	34.78	31.96	34.38	**29.86**	33.14
Exergy destruction (GJ/t_{NH3})	**9.64**	25.26	30.75	26.75	**34.13**	28.47
Extended exergy destruction (GJ/t_{NH3})[1]	**12.81**	33.96	39.00	34.61	**43.36**	36.79

1.Overall exergy consumption increases if the cumulative efficiency of the electricity grid (55.67%), natural gas (91.09%) and bagasse (86.13%) supply are considered as in [49, 50].

By comparing the *extended exergy efficiency* and the standalone ammonia plant efficiency (i.e. *not extended*), the performance is appreciably impaired (8.9-15.2%) when the irreversibility present in the upstream feedstock supply chains is incorporated. These figures are of course dependent on other process externalities such as the transportation and distribution infrastructure, the production efficiency of the energy resources as well as the composition of the electricity mix concerned. It is important to mention other scenarios which recently have earned attention in Brazil to mitigate the fossil fuel consumption in the ammonia production process, which consider the syngas production by using the steam reforming of ethanol, encouraged by a well-established sugarcane ethanol economy [52-56].

Finally, it must be noticed that, lower electricity selling prices should promote the integration of improved energy recovery and conversion systems (i.e. waste heat upgraded to useful input), since the *fuel consumption* in the internal cogeneration unit should attempt to compensate the improved performance of the external electricity generation in the grid. Paradoxically, higher purchasing electricity and natural gas prices are also necessary to encourage the rational transformation of the waste heat exergy into mechanical power by using cogeneration, since imported electricity cost becomes prohibitively high. Accordingly, it can be shown that the relative prices of the electricity and the fuels imported play a decisive role when determining the pathway that the economic optimization of the industrial process must follow. Other important factors comprise the exergy efficiency of the electricity generation in both the national electricity mix and in the autonomous CHP production system, which, in turn, depends on the technologies composing the superstructure considered (e.g. steam network or combined cycle). Equations (21-22) show the thermoeconomy balances of the cogeneration system and the chemical plant, respectively, shown in Fig. 10:

$$c_{NG}B_{NG} + c_{SG}B_{SG} + c_{Q}B_{Q} + Z_{cogen} = c_{power}B_{power} + c_{steam}B_{steam} \tag{21}$$

$$c_{power}B_{power} + c_{steam}B_{steam} + c_{EE}B_{EE} + c_{Biomass}B_{Biomass} + Z_{Chem.} = c_{SG}B_{SG} + c_{Q}B_{Q} + c_{\mathrm{Product}}B_{\mathrm{Product}} \tag{22}$$

where c [euro/kWh] and B [kW] stands for the unit thermoeconomy cost and the exergy flow rate, respectively, of the energy resources involved, namely natural gas (NG), syngas (SG), waste heat (Q),

electricity (EE), biomass, power and steam. Moreover, the annualized capital cost can be used to calculate the investment cost rate Z [euro/h].

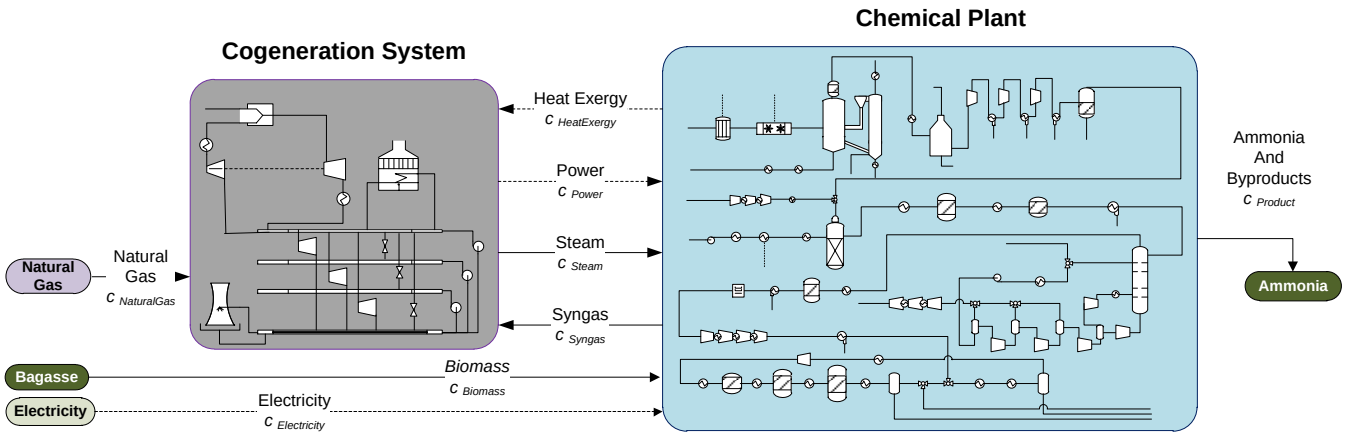

Fig. 10. Thermoeconomy balance of the cogeneration unit and the chemical plant.

Thus, by setting the ratio between the prices of the natural gas consumed and the electricity imported (in this study, $c_{NG} : c_{EE}$ = 0.032 euro/kWh$_{GN}$: 0.108 euro/kWh$_{EE}$ = 0.296), the complex relationship that governs the costs formation of the inputs and products of the chemical and the cogeneration plants can be evidenced from Eq.(23):

$$\frac{\mathbf{c_{NG}}}{\mathbf{c_{EE}}} = \frac{\mathbf{c_{power}} B_{power} + c_{steam} B_{steam} - c_{SG} B_{SG} - c_Q B_Q - Z_{cogen}}{c_{SG} B_{SG} + c_Q B_Q + \mathbf{c_{Product}} B_{Product} - c_{Biomass} B_{Biomass} - \mathbf{c_{power}} B_{power} - c_{steam} B_{steam} - Z_{Chem.}} \cdot \frac{B_{EE}}{B_{NG}} = 0.296 \quad (23)$$

This intricate interplay strongly influences the choice of importing an additional amount of natural gas (B_{NG}) for autonomously producing power (B_{power}) *over* the direct import of electricity from the grid (B_{EE}). In this way, provided that the cost of the electricity produced in the cogeneration system, c_{power}, is lower than that of the electricity imported form the grid, c_{EE} (whereas the cost of the natural gas and the bagasse are set as constant), the utilization of natural gas as fuel in the cogeneration system results thermoeconomically more attractive than importing electricity. However, the economic trade-off is not limited to choosing between importing electricity or fuel from the market, as it also depends on the potential of self-generating the power required throughout the plant by consuming syngas as fuel. Thus, the performance of the syngas production, purification and conversion systems adds further complexity to the optimization problem, as it has been demonstrated by the highest operating revenues obtained in this work. Additionally, the higher the amount of syngas consumed, the lower the quantity of value added products (i.e. ammonia) is produced. This circumstance explains why better solutions in terms of exergy efficiency, product yield or reduced environmental impact are not necessarily meant to be as well the most profitable ones in an specific basis [41].

Indeed, in the short and middle term, the global production of these important commodities (fertilizers, transportation fuels, bulk chemicals) is foreseen to remain dominated by the use of the non-renewable natural gas resources, especially coal and natural gas. Yet, in spite of the current shortcoming related

to the high investment risk and the less mature energy conversion technologies of biomass, further efforts on research and development on the renewable energy sources conversion will eventually increase the introduction of alternative production routes at larger scales in the SNF industry.

5. Conclusions

In this work, a conventional natural gas-based ammonia production plant is compared with a set of alternative biomass-based ammonia production facilities, aiming to reduce the amount of non-renewable exergy consumed, whereas increasing the operating revenues. The combined energy integration and exergy analyses performed allowed spotting the best alternatives of utility systems that increase the revenues, while maximizing the recovery of the available waste heat exergy. As a result, the exergy efficiencies of the natural and biomass-based ammonia production plant average 65.8% and 41.3%, respectively, whereas the overall emission balance varies from 0.5 to -2.3 t_{CO2}/t_{NH3}, respectively. The negative values point towards the environmental benefits brought about by the production of chemicals through the use of alternative energy sources such as biomass. However, in the short to medium terms, the global production of these important commodities is foreseen to remain dominated by the use of the non-renewable natural gas resources, especially coal and natural gas. Yet, further efforts on research and development of more efficient conversion technologies of renewable energy sources must look towards the introduction of alternative ammonia production routes at larger scales in the SNF industry, in spite of the current high investment risk and less mature energy conversion technologies of biomass. Moreover, the electricity import, whether available, may help reducing the extent of the irreversibility in the biomass-based ammonia production, as well as reducing the overall CO_2 emissions. However, higher operating revenues can be rather achieved by totally replacing the costly natural gas input and avoiding the electricity import, thus, favoring the consumption of the syngas produced in a combined power cycle for supplying the heat and power demands. Finally, it must be noticed that by defining an extended plant consumption and efficiency concepts, the whole effect of the production process, including the inefficiencies of upstream feedstock supply chain can be evaluated. The results show to be strongly dependent on the indirect emissions, the energy resources used (natural gas, electricity or bagasse) and the ratio of the price of electricity to natural gas adopted.

Acknowledgments

The first author would like to acknowledge the National Agency of Petroleum, Gas and Biofuels – ANP and its Human Resources Program (PRH/ANP Grant 48610.008928.99), Swiss Government Excellence Scholarship Program (Grant 2016.0876), and the Colombian Administrative Department of Science, Technology and Innovation – COLCIENCIAS. Third author would like to thank National Research Council for Scientific and Technological Development, CNPq (grant 304935/2016-6).

References

1. IPTS, *Reference Document on Best Available Techniques for the Manufacture of Large Volume Inorganic Chemicals - Ammonia, Acids and Fertilisers Industries*. 2007, Integrated Pollution Prevention and Control
2. FAO, *World fertilizer trends and outlook to 2018*. 2015: Rome.

3. Florez-Orrego, D., Nascimento Silva, F., Oliveira Jr., S. *Syngas Production with Thermo-Chemically Recuperated Gas Turbine Systems: An Exergy Analysis and Energy Integration Study*. in *31th International Conference on Efficiency, Cost, Optimization, Simulation and Environmental Impact of Energy Systems - ECOS 2018, June 17th - 22nd*. 2018. Guimaraes, Portugal: University of Minho.
4. Flórez-Orrego, D., Oliveira Junior, S., *On the efficiency, exergy costs and CO2 emission cost allocation for an integrated syngas and ammonia production plant.* Energy, 2016. **117, Part 2**: p. 341-360.
5. Frattini, D., Cinti, G., Bidini, G., Desideri, U., Cioffi, R., Jannelli, E., *A system approach in energy evaluation of different renewable energies sources integration in ammonia production plants.* Renewable Energy, 2016. **99**: p. 472-482.
6. Arora, P., Hoadley, A., Mahajani, S., Ganesh, A., *Multi-objective optimization of biomass based ammonia production - Potential and perspective in different countries.* Journal of Cleaner Production, 2017. **148**: p. 363-374.
7. Hannula, I., *Hydrogen production via thermal gasification of biomass in near-to-medium term.* 2009, VTT Technical Research Centre of Finland.
8. Kurkela, E., Nieminen, M., Simell, P. *Development and commercialization of biomass and waste gasification technologies from reliable and robust co-firing plants towards synthesis gas production and advanced power cycles*. in *2nd World Conference and Technology Exhibition on Biomass for Energy, Industry and Climate Protection, ETA - Florence, WIP - Munich*. 2004. Florence, Italy.
9. Gilbert, P., Alexander, S., Thornley, P., Brammer, J., *Assessing economically viable carbon reductions for the production of ammonia from biomass gasification.* Journal of Cleaner Production, 2014. **64**: p. 581-589.
10. Santos, V.E.N., Ely, R. N., Szklo, A. S., Magrini, A., *Chemicals, electricity and fuels from biorefineries processing Brazil's sugarcane bagasse: Production recipes and minimum selling prices.* Renewable and Sustainable Energy Reviews, 2016. **53**: p. 1443-1458.
11. Andersson, J., Lundgren, J., *Techno-economic analysis of ammonia production via integrated biomass gasification.* Applied Energy, 2014. **130**: p. 484-490.
12. Hamelinck, C., Faaij, A.P.C., *Future prospects for production of methanol and hydrogen from biomass.* Journal of Power Sources, 2002. **111**(1): p. 1-22.
13. NETL. *Gasification Background, Markets for Gasification*, 2014, Accessed 29.10.2017; Available from: https://www.netl.doe.gov/research/coal/energy-systems/gasification/gasifipedia/markets.
14. Ett, G., Landgraf, F., Derenzo, S., Yu, A., Reis, L., Mazzonetto, A., Antonoff, H., Souza, L., *Brazilian Bio Fuels Production Scenario (Biogas, Biomethane and Biosyngas)*, in *International Seminar on Biomass, Biogas and Energy Efficiency - Regional Leaders Summit*. 2013: Sao Paulo, Brazil.
15. Ett, G., Landgraf, F., Sin Yu, A., Nunis, A., Poco, J., Silveira, J., Derenzo, S., *Biosyngas - Biomass entrained flow gasfication*, in *5th International Conference on Engineering for Waste and Biomass Valorization*. 2014: RJ, Brazil.
16. Camacho-Ardila, Y., Figueroa, J., Lunelli, B., Maciel Filho, R., Wolf Maciel, M. *Syngas production from sugar cane bagasse in a circulating fluidized bed gasifier using Aspen PlusTM: Modelling and Simulation*. in *2nd European Symposium on Computer Aided Process Engineering*. 2012. London, UK: Elsevier.
17. Marques, F., *Bagasse is the target.* Revista Pesquisa FAPESP, 2009 (Special issue May 2009/Dec 2010): p. 32-36.
18. Reddy, N., Yang, Y., *Fibers from Sugarcane Bagasse*, in *Innovative Biofibers from Renewable Resources*, N. Reddy and Y. Yang, Editors. 2015, Springer Berlin Heidelberg: p. 29-30.
19. Tock, L., Maréchal, F., Perrenoud, M., *Thermo-environomic evaluation of the ammonia production.* The Canadian Journal of Chemical Engineering, 2015. **93**(2): p. 356-362.
20. Florez-Orrego, D., Sharma, S., Oliveira Jr, S., Marechal, F. *Combined Exergy Analysis and Energy Integration for Design Optimization of Nitrogen Fertilizer Plants*. in *30th International Conference on Efficiency, Cost, Optimization, Simulation and Environmental Impact of Energy Systems, ECOS 2017, July 2 - 6* 2017. San Diego, United States of America: San Diego State University.
21. Leites, I.L., Sama, D. A., Lior, N., *The theory and practice of energy saving in the chemical industry: some methods for reducing thermodynamic irreversibility in chemical technology processes.* Energy, 2003. **28**(1): p. 55-97.
22. Hou, K., Hughes, R., *The kinetics of methane steam reforming over a Ni/-Al2O3 catalyst.* Chemical Engineering Journal, 2001. **82**: p. 311-328.
23. Appl, M., *Ullmann's encyclopedia of industrial chemistry, Vol.11. Chapter 2.*, 2012, Wiley-VCH GmbH, Weinheim.
24. Flórez-Orrego, D., Oliveira Junior, S., *Exergy assessment of single and dual pressure industrial ammonia synthesis units.* Energy, 2017. **141**: p. 2540-2558.
25. Basu, P., *Biomass Gasification and Pyrolysis: Practical Design*. 2010: Academic Press.
26. Vitasari, C.R., Jurascik, M., Ptasinski, K., *Exergy analysis of biomass-to-synthetic natural gas (SNG) process via indirect gasification of various biomass feedstock.* Energy, 2011. **36**(6): p. 3825-3837.
27. Juraščík, M., Sues, A., Ptasinski, K., *Exergy analysis of synthetic natural gas production method from biomass.* Energy, 2010. **35**(2): p. 880-888.

28. Kinchin, C.M., Bain, R.L., *Hydrogen Production from Biomass via Indirect Gasification: The Impact of NREL Process Development Unit Gasifier Correlations, Technical Report NREL/TP-510-44868, May 2009*. NREL.
29. Spath, P.L., Dayton, D.C. , *Preliminary Screening - Technical and Economic Assessment of Synthesis Gas to Fuels and Chemicals with Emphasis on the Potential for Biomass-Derived Syngas. NREL/TP-510-34929*. 2003, National Renewable Energy Laboratory: Golden, Colorado. p. 160.
30. Couper, J., Penney, W. R., Fair, J. R., Walas, S. M., *Chemical Process Equipment (Third Edition)*. 2012, Boston: Butterworth-Heinemann.
31. Maréchal, F., Kalitventzeff, B., *Identification of the optimal pressure levels in steam networks using integrated combined heat and power method.* Chemical Engineering Science, 1997. **52**(17): p. 2977-2989.
32. ASPENTECH, *Aspen Physical Property System - Physical Property Methods V7.3 - User Guide*. 2011.
33. Abdollahi-Demneh, F., Moosavian, M., Omidkhah, M., Bahmanyar, H., *Calculating exergy in flowsheeting simulators: A HYSYS implementation.* Energy, 2011. **36**(8): p. 5320-5327.
34. Puig-Arnavat, M., Bruno, J., Coronas, A., *Modified Thermodynamic Equilibrium Model for Biomass Gasification: A Study of the Influence of Operating Conditions.* Energy & Fuels, 2012. **26**(2): p. 1385-1394.
35. Gomez-Barea, A., Nilsson, S., Vidal Barrero, F., Campoy, M., *Devolatilization of wood and wastes in fluidized bed.* Fuel Processing Technology, 2010. **91**(11): p. 1624-1633.
36. Duret, A., Friedli, C., Maréchal, F., *Process design of Synthetic Natural Gas (SNG) production using wood gasification.* Journal of Cleaner Production, 2005. **13**(15): p. 1434-1446.
37. Doherty, W., Reynolds, A., Kennedy, D., *The effect of air preheating in a biomass CFB gasifier using ASPEN Plus simulation.* Biomass and Bioenergy, 2009. **33**(9): p. 1158-1167.
38. Szargut, J., Morris, D, Steward, F, *Exergy analysis of thermal, chemical, and metallurgical processes*. 1988, New York: Hemisphere Publishing Corporation.
39. Channiwala, S., Parikh, P., *A unified correlation for estimating HHV of solid, liquid and gaseous fuels.* Fuel, 2002. **81**(8): p. 1051-1063.
40. Keller, A., Viswanathan, S., *Integrated pressurized steam hydrocarbon reformer and combined cycle process*, US 8,375,725 B2, U.S.Patent Office, 2013, Phillips 66 Company, Houston, TX (US): United States.
41. Kalitventzeff, B., Maréchal, F., Closon, H., *Better solutions for process sustainability through better insight in process energy integration.* Applied Thermal Engineering, 2001. **21**(13–14): p. 1349-1368.
42. Ingham, A., *Reducing the Carbon Intensity of Methanol for Use as a Transport Fuel.* Johnson Matthey Technology Review, 2017. **61**(4): p. 297-307.
43. ASPENTECH, *Aspen Plus V8.8, Aspen technology Inc.* 2015: Bedford, United States.
44. Yoo, M., Lessard, L, Kermani, M., Maréchal, F. *OSMOSE Lua: A Unified Approach to Energy Systems Integration with Life Cycle Assessment*. in *12th International conference PSE 2015 and 25th International conference ESCAPE* 2015. Copenhagen, Denmark.
45. Maréchal, F., Kalitventzeff, B., *Process integration: Selection of the optimal utility system.* Computers & Chemical Engineering, 1998. **22**: p. S149-S156.
46. Linnhoff, B., Hindmarsh, E., *The pinch design method for heat exchanger networks.* Chemical Engineering Science, 1983. **38**(5): p. 745-763.
47. Hotza, D., Diniz da Costa, J. C., *Fuel cells development and hydrogen production from renewable resources in Brazil.* International Journal of Hydrogen Energy, 2008. **33**(19): p. 4915-4935.
48. Gassner, M., Maréchal, F., *Increasing Efficiency of Fuel Ethanol Production from Lignocellulosic Biomass by Process Integration.* Energy & Fuels, 2013. **27**(4): p. 2107-2115.
49. Flórez-Orrego, D., Silva, J. A. M., Oliveira Jr, S., *Renewable and non-renewable exergy cost and specific CO2 emission of electricity generation: The Brazilian case.* Energy Conversion and Management, 2014. **85**: p. 619-629.
50. Flórez-Orrego, D., Silva, J.A.M., Velásquez, H., Oliveira Jr., S., *Renewable and non-renewable exergy costs and CO2 emissions in the production of fuels for Brazilian transportation sector.* Energy, 2015. **88**: p. 18-36.
51. Flórez-Orrego, D., Silva, J. A. M., Oliveira Jr, S., *Exergy and environmental comparison of the end use of vehicle fuels: The Brazilian case.* Energy Conversion and Management, 2015. **100**: p. 220-231.
52. Caetano de Souza, A., Luz-Silveira, J., Sosa, M., *Physical-Chemical and Thermodynamic Analyses of Ethanol Steam Reforming for Hydrogen Production.* Journal of Fuel Cell Science and Technology, 2006. **3**(3): p. 346-350.
53. Silveira, J., Souza, A., Silva, M., *Thermodynamic Analysis of Direct Steam Reforming of Ethanol in Molten Carbonate Fuel Cell.* Journal of Fuel Cell Science and Technology, 2008. **5**(2): p. 021012-021012.
54. BNDES, *Bioetanol de cana-de-açúcar: Energia para o desenvolvimento sustentável*. 2008, Rio de Janeiro: BNDES.
55. Rossi, C., Alonso, C., Antunes, O., Guirardello, R., Cardozo-Filho, L., *Thermodynamic analysis of steam reforming of ethanol and glycerine for hydrogen production.* International Journal of Hydrogen Energy, 2009. **34**(1): p. 323-332.

56. Lima da Silva, A., Malfatti, C., Müller, I., *Thermodynamic analysis of ethanol steam reforming using Gibbs energy minimization method: A detailed study of the conditions of carbon deposition*. International Journal of Hydrogen Energy, 2009. **34**(10): p. 4321-4330.